

Differential developmental trajectories of magnetic susceptibility in human brain gray and white matter

Wei Li¹, Bing Wu², Anastasia Batrachenko¹, Christian Langkammer³, Stefan Ropele³, Rajendra Morey^{1,4}, Vandana Shashi⁵, Allen W. Song^{1,6}, and Chunlei Liu^{1,6}
¹Brain Imaging & Analysis Center, Duke University, Durham, North Carolina, United States, ²GE Healthcare China, Beijing, China, ³Neurology, Medical University of Graz, Graz, Austria, ⁴Psychiatry and Behavioral Sciences, Durham VA Medical Center, Durham, North Carolina, United States, ⁵Pediatrics, Duke University, Durham, North Carolina, United States, ⁶Radiology, Duke University, Durham, North Carolina, United States

TARGET AUDIENCE: This study is targeted to researchers interested in using magnetic susceptibility as a tool to investigate the alterations in brain tissue chemical composition in various neurological diseases, especially those related to brain demyelination or iron deposition.

PURPOSE: Magnetic susceptibility provides excellent contrast between gray and white matter, which has been shown to be highly correlated with tissue chemical composition, especially iron and myelin (1, 2). Proper iron metabolism and myelination are essential for normal brain functioning. As the myelination and iron deposition of brain gray and white matter evolves both temporally and spatially, the age-related susceptibility changes may provide valuable information regarding the physiological state of the human brain. In this work, we measured magnetic susceptibility of human brains *in vivo* ranging from 1 to 83 years old, aiming for providing a reference of the evolutions of magnetic susceptibility in different anatomical and functional regions due to normal brain development and ageing.

MATERIALS AND METHODS: *Brain Imaging:* A total of 181 subjects were included. While the subjects of 7 years and older were healthy (age 7-83 y/o, n = 174), the children (age 1-5 y/o, n = 7) were diagnosed with cerebral palsy (CP). The inclusion of CP subjects introduced heterogeneity into the population. However, it was necessary to obtain information of early brain development, since consenting infants and children for MRI study is difficult if without any clinical benefits. To minimize the impact of non-homogeneous population, only hemiplegic CP was included, and the analysis was performed on the normal appearing hemisphere. All subjects were scanned at 3T, using single- or multi-echo gradient echo sequences. The in-plane resolution was 0.9 or 1 mm, and the slice thickness was 1-4 mm.

Data Analysis: Phase images from different coils were unwrapped using a Laplacian-based method and combined (3). The background phase was removed with a modified SHARP approach (1, 3), and normalized to yield the frequency shift, which is independent of the scan parameters. The tissue frequency shift was used for susceptibility mapping with the LSQR method (3). Region of interests (ROIs), including the a few major subcortical white matter bundles, cortical regions and iron-rich deep nuclei, were manually outlined (Fig. 1). The background phase removal procedure essentially set the reference susceptibility to the mean brain tissue susceptibility. Hence, susceptibility values from selected ROIs were directly used for analysis. In addition, R² values from the same ROI as susceptibility were also evaluated for the iron rich nuclei.

RESULTS: Brain gray and white matter show significantly different developmental trajectories of magnetic susceptibility (Fig. 2). In both cortical and subcortical white matter, an initial decrease followed by a subsequent increase of magnetic susceptibility was observed, which could be fitted by the following Poisson curve (Table 1):

$$\chi = A \cdot \text{age} \cdot \exp(-B \cdot \text{age}) + C \quad [1]$$

where A, B and C are tissue specific parameters. The same Poisson curve has been used previously by Lebel et al to describe the changes of diffusion parameters over the lifespan (4). As age increases, magnetic susceptibility of various white matter groups shows different evolution patterns, with peak ages varying from 25 to 46 years.

In contrast, in the gray matter, including the cortical gray matter and the iron-rich deep nuclei, magnetic susceptibility displays a monotonic increase, which can be described with the exponential growth (Table 2):

$$\chi = \alpha \cdot [1 - \exp(-\beta \cdot \text{age})] + \gamma \quad [2]$$

where α , β and γ are tissue specific parameters. This exponential growth model was proposed by Hallgren and Sourander (5) for the age-related iron content changes. The rate of susceptibility increase in different gray matter regions is also different. For example, the rate of increase in GP and SN dramatically reduces with age (larger β values), while the rate remains nearly constant in SC, MC, PU and DN (very small β values). The same evolution pattern with similar time parameter β were observed for the changes of R² over the lifespan.

DISCUSSION: In this study, profound changes of magnetic susceptibility were observed in both brain white matter and gray matter. The Poisson trajectories describing the susceptibility of the white matter are consistent with the known knowledge of brain myelination during brain maturation and ageing, observed from DTI studies (4). According to Bartzokis, the maturation and breakdown of myelin in the human brain are essentially determined by oligodendrocytes, which are responsible for the generation of myelin sheath. Oligodendrocytes are likely the most vulnerable cell types to be affected during normal brain ageing, and the alterations in the amount and the activities of oligodendrocytes would predict biphasic patterns of brain myelination (6). The exponential growth of susceptibility contrast in gray matter is also in good agreement with the knowledge of iron deposition and R² changes (5). These results suggested that susceptibility imaging may provide a promising tool for assessment of myelination and iron content. In turn, an improved understanding of the spatial and temporal patterns of myelination and iron deposition during brain maturation and ageing may allow for better utilization of susceptibility contrast for clinical evaluation of various neurological diseases, for example, multiple sclerosis, Parkinson's diseases, and so on.

REFERENCES: (1) Schweser et al, NeuroImage, 2011. (2) Liu et al, NeuroImage, 2011. (3) Li et al, NeuroImage 2011. (4) Lebel et al, NeuroImage, 2012. (5) Hallgren & Sourander, J Neurochem. 1958. (6) Bartzokis, Neurobiol. Aging, 2004.

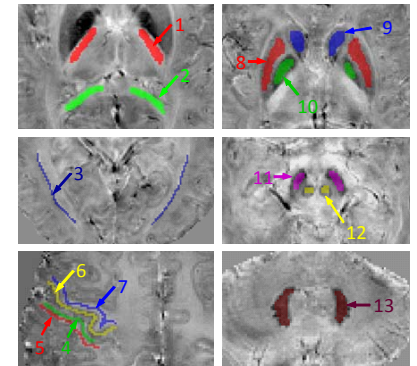


Fig. 1. Region of interests. 1: internal capsule (IC); 2: splenium of corpus callosum (SCC); 3: optic radiation (OR); 4: sensory cortex (SC); 5: sensory cortex white matter (SC-WM); 6: motor cortex (MC); 7: motor cortex white matter (MC-WM); 8: putamen (PU); 9: caudate nucleus (CN); 10: globus pallidus (GP); 11: substantia nigra (SN); 12: red nucleus (RN); 13: dentate nucleus (DN).

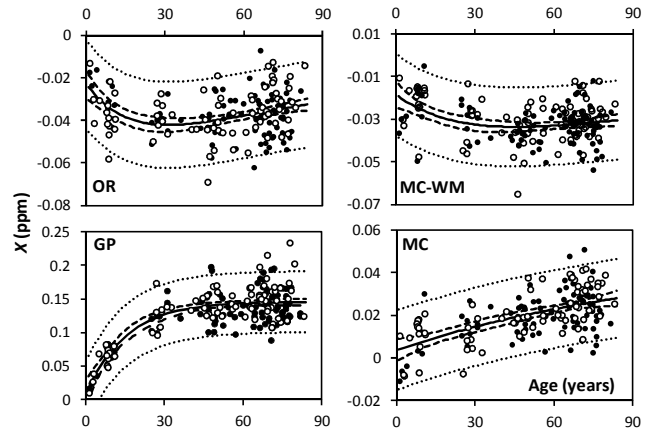


Fig. 2. Evolution of magnetic susceptibility in representative gray and white matter regions. Open circle: male, close circle: female.

Table 2. Age-related susceptibility and R² changes in gray matter

| | χ (ppm) vs. age (year) | R ² (sec ⁻¹) vs. age (year) |
|----|--|---|
| SC | $\chi = 0.615 \cdot [1 - \exp(-3 \cdot 10^{-3} \cdot \text{age})] + 0.005$ | - |
| MC | $\chi = 0.044 \cdot [1 - \exp(-0.010 \cdot \text{age})] + 0.004$ | - |
| PU | $\chi = 0.243 \cdot [1 - \exp(-0.008 \cdot \text{age})] - 0.001$ | $R^2 = 36.4 \cdot [1 - \exp(-0.013 \cdot \text{age})] + 12.8$ |
| GP | $\chi = 0.139 \cdot [1 - \exp(-0.065 \cdot \text{age})] + 0.007$ | $R^2 = 31.2 \cdot [1 - \exp(-0.069 \cdot \text{age})] + 10.0$ |
| CD | $\chi = 0.081 \cdot [1 - \exp(-0.031 \cdot \text{age})] + 0.006$ | $R^2 = 18.3 \cdot [1 - \exp(-0.023 \cdot \text{age})] + 12.0$ |
| RN | $\chi = 0.117 \cdot [1 - \exp(-0.058 \cdot \text{age})] - 0.023$ | $R^2 = 30.2 \cdot [1 - \exp(-0.007 \cdot \text{age})] + 5.4$ |
| SN | $\chi = 0.117 \cdot [1 - \exp(-0.099 \cdot \text{age})] - 0.012$ | $R^2 = 34.1 \cdot [1 - \exp(-0.082 \cdot \text{age})] + 4.9$ |
| DN | $\chi = 0.121 \cdot [1 - \exp(-0.026 \cdot \text{age})] + 0.002$ | $R^2 = 27.5 \cdot [1 - \exp(-0.034 \cdot \text{age})] + 13.4$ |

Table 1. Age-related susceptibility changes in white matter

| | χ (ppm) vs. age (year) | peak age (year) |
|-------|---|-----------------|
| IC | $\chi = -0.0015 \cdot \text{age} \cdot \exp(-0.022 \cdot \text{age}) - 0.032$ | 44.5 ± 8.4 |
| SCC | $\chi = -0.0022 \cdot \text{age} \cdot \exp(-0.030 \cdot \text{age}) + 0.001$ | 33.8 ± 4.6 |
| OR | $\chi = -0.0017 \cdot \text{age} \cdot \exp(-0.032 \cdot \text{age}) - 0.023$ | 31.5 ± 5.8 |
| SC-WM | $\chi = -0.0021 \cdot \text{age} \cdot \exp(-0.039 \cdot \text{age}) - 0.015$ | 25.4 ± 5.1 |
| MC-WM | $\chi = -0.0009 \cdot \text{age} \cdot \exp(-0.022 \cdot \text{age}) - 0.018$ | 45.6 ± 13.6 |